EEG findings in CART T associated neurotoxicity: clinical and radiological correlations

Isabelle Beuchat, MD, Husain Danish, MD, Daniel B. Rubin, MD, PhD, Caron Jacobson, MD, Matthew Robertson, MD, Henrikas Vaitkevicius, MD, Jong Woo Lee, MD, PhD

Department of Neurology, Brigham and Women's Hospital, Harvard School of Medicine, Boston, MA, USA (IB, DH, DR, HV, JWL)
Department of Neurology, Massachusetts General Hospital, Harvard Medical School, Boston, MA, USA (DR, DH)
Dana Farber Cancer Institute, Harvard Medical School, Boston, MA, USA (CJ)
Division of Nuclear Medicine, Department of Radiology, Brigham and Women's Hospital, Harvard Medical School, Boston, MA, USA (MR)

Corresponding author
Jong Woo Lee, MD, PhD
Associate Professor of Neurology
The Edward B. Bromfield Epilepsy Program
Brigham and Women's Hospital
60 Fenwood Rd
Boston, MA 02115
jlee38@bwh.harvard.edu
617-732-7547 (p)
617-730-2885 (f)

Funding: IB received a Postdoctoral Mobility Fellowship from the Swiss National Science Foundation.

Conflict of interest:
IB and HD have no conflicts. DR reports consulting for Celgene. CJ reports consulting for Kite, Novartis, BMS, Celgene, Nkarta, Lonza, Precision Biosciences, Abbvie, and research funding from Pfizer. MR has no conflicts. HV has no conflicts relevant to this article, this work was conceived and completed while he was working at Brigham and Women's Hospital, since then, he has been employed by Marinus Pharmaceutical Inc.JWL 1) Bioserenity (contract work), Teladoc (contract work), Biogen (consultant), Soterya (co-founder), Engage Therapeutics (site PI), NINDS (site PI).

Authorship statement: Conception and design of the study: IB, HD, HV, JWL. Acquisition of data: IB, HD, HV, DR, JWL. Data analysis: IB, JWL. Drafted and revised the manuscript for intellectual content: IB, HD, HV, DR, JWL.

Abstract

Background

While EEG is frequently reported as abnormal after CAR T cell therapy, its clinical significance remains unclear. We aim to systematically describe EEG features in a large single-center cohort and correlate them with clinical and radiological findings.

Methods

We retrospectively identified patients undergoing CAR T cell therapy who had continuous EEG. Neurotoxicity grades, detailed neurological symptoms, and brain MRI or FDG-PET were obtained. Correlation between clinical and radiological findings and EEG features was assessed.

Results

In 81 patients with median neurotoxicity grade 3 (IQR 2-3), diffuse EEG background slowing was the most common finding and correlated with neurotoxicity severity ($p < 0.001$). A total of 42 patients had rhythmic or periodic patterns, 16 of them within the ictal-interictal-continuum (IIC), 5 with clinical seizures, and 3 with only electrographic seizures. Focal EEG abnormalities, consisting of lateralized periodic discharges (LPD, n=1), lateralized rhythmic delta activity (LRDA, n=6), or focal slowing (n=19), were found in 22 patients. All patients with LRDA, LPD, and 10/19 patients with focal slowing had focal clinical symptoms concordant with these EEG abnormalities. In addition, these focal EEG changes often correlated with PET hypometabolism or MRI hypoperfusion, in absence of a structural lesion.

Conclusion

In adult patients experiencing neurotoxicity after CAR T cell infusion, EEG degree of background disorganization correlated with neurotoxicity severity. IIC patterns and focal EEG abnormalities are frequent and often correlate with focal clinical symptoms and with PET-hypometabolism/MRI-hypoperfusion, without structural lesion. The etiology of these findings remains to be elucidated.

Keywords: CAR T cell, ICANS, neurotoxicity, EEG, PET

Key Points

1. The degree of EEG background slowing correlates with neurotoxicity severity
2. Patterns within the ictal-interictal continuum and focal EEG abnormalities are often found
3. Focal EEG changes correlate with clinical symptoms and PET-hypometabolism/MRI-hypoperfusion

Importance of the study

Cellular immunotherapy with chimeric antigen receptor (CAR) T cells has demonstrated impressive results in the treatment of relapsed or refractory hematological malignancies. However, treatment is often complicated by acute neurotoxicity, the presentation of which is varied and can involve both focal and generalized symptoms. Despite its high morbidity, the underlying pathophysiology of CAR-T cell therapy-related neurotoxicity remains poorly understood. As CAR T cells become more widely used, recognition and understanding of their unique neurological toxicities are critical.

Here we provide detailed EEG descriptions, in correlation with clinical and radiological data, to help clinicians better understand what to expect in this unique population. Our data suggest that EEG background alteration correlates with neurotoxicity grades. Further prospective studies should investigate the possibility of using EEG to monitor neurotoxicity severity. Furthermore, patterns within the ictal-interictal-continuum and EEG focal abnormalities were frequently observed. Patients with these focal EEG patterns often presented with focal neurological symptoms and unexpected PET hypometabolism or MRI hypoperfusion, without MRI structural lesions. These focal findings raise yet unanswered questions regarding neurotoxicity pathophysiology.

Introduction

Cellular immunotherapy with chimeric antigen receptor (CAR) T cells shows excellent therapeutic responses in refractory hematologic malignancies [1,2]. CAR T cells consist of autologous or allogenic T-cells genetically modified to express chimeric antigen receptors that recognize a specific tumor antigen [3]. Although numerous clinical trials demonstrated impressive results[1,4,5] one of the main challenges remain the management and understanding of their acute toxicities: cytokine release syndrome (CRS) and neurotoxicity [6-9]. CRS is characterized by high fever, hypotension, hypoxia, and, in more severe cases multi-system organ dysfunction. CRS typically occurs during the first week after treatment, as a result of inflammatory cytokines released as the infused CAR T cells undergo rapid expansion [5,10,11]. Interleukin 6 (IL-6) receptor blockade (tocilizumab) is recommended for moderate to severe CRS treatment, as it can effectively mitigate CRS symptoms in most patients, without impairing the short-term efficacy of CAR T therapy [5,9,10,12].

In contrast to CRS, neurotoxicity remains poorly understood. At least one neurological symptom is described in up to 77% of the patients with large variability of neurotoxicity grades reported across studies, possibly confounded by the use of different grading scales [7-9,13,14]. Recently, the American Society for Transplantation and Cellular Therapy (ASTCT) introduced the term “immune effector cell-associated neurotoxicity syndrome” (ICANS) and proposed a uniform grading scale with a consensus tool for encephalopathy grading (ICE score) [7]. Global encephalopathy with delirium, mental status change, and/or language impairment is the most frequent neurological sign. However, a large range of symptoms have been reported, including, but not limited to, tremor, epileptic seizures, focal neurological signs such as aphasia or focal weakness, cerebral edema, and death [9,10,15,16]. Neurotoxicity typically occurs during the first week after infusion, in the setting of ongoing or resolving CRS [9,17,18]. As rapid clinical progression despite treatment has been described, close monitoring and early admission to a critical care unit are recommended [1,6,16]. Treatment is currently limited to steroids and seizure management, although IL-1, IL-6, and JAK targeting therapies are being considered.

Although no large studies have been reported to date, EEGs are frequently reported as abnormal in this population [9,13,19-22]. Diffuse background slowing or loss of posterior rhythm (PDR) are the most frequently described abnormalities [9,19,21,22]. Several other EEG abnormalities including focal slowing and/or attenuation and ictal-interictal continuum (IIC) patterns, such as rhythmic or periodic pattern (RPP) have also been reported [9,20,21]. The clinical significance of these EEG patterns remains unclear, and the frequency of seizures is variable among studies. One of the first major studies reported 30% (15/53) seizure rate in

patients treated with CAR T cells with up to 48% (16/733) of the patients presenting with neurotoxicity experiencing seizures [22]. This observation has led to the recommendation of antiseizure prophylaxis in CAR T patients. However, the seizure occurrence rate is difficult to formally establish with later studies reporting seizures' incidence ranging between 0-10% of all patients receiving CAR T and between 1-30% of the ones presenting with neurotoxicity [9,15,21,23-27]. Few EEG data are available with only a handful of electrical seizures or status epilepticus reported [9,13,19,21,22]. Furthermore, several authors reported "ictal-looking" clinical events such as involuntary rhythmic movements, myoclonus, sudden changes in speech, focal deficit, facial automatism without EEG correlates, and with normal structural MRI [21,22].

We aim to systemically describe EEG features in a large cohort of CAR T cell therapy-related neurotoxicity, to assist clinicians to better understand EEG findings in this unique population. Secondly, we aim to investigate the relationship between EEG abnormalities and clinical symptoms of neurotoxicity with the hypothesis that higher neurotoxicity grades may correlate with increased EEG background alteration, and that focal EEG abnormalities may be accompanied by contralateral focal neurological deficits. Finally, we aim to investigate if EEG patterns in the IIC are associated with higher neurotoxicity grades.

Material and Methods

Patients

Using the Critical Care EEG Monitoring Research Consortium (CCEMRC) EEG database, we retrospectively identified every adult patient receiving CAR T cell treatment who underwent continuous EEG monitoring between May 2016 and January 2020 at the Brigham and Women's Hospital. Treatment inclusion, exclusion criteria, and patients' management have previously been described [9]. Patients were assessed daily for CRS (according to Lee [28]) and neurotoxicity (according to the National Cancer Institute Common Terminology Criteria for Adverse Effects v4.0 [29]), by an inpatient oncologist and consulting neurologist. An adapted version of the Common Terminology Criteria for Adverse Events (CTCAE) was used in our center, in which isolated headaches were not considered neurotoxicity. To improve generalization with other studies, patients who presented with any clinical seizures were retrospectively considered as having neurotoxicity at least grade 3. Date of onset, peak and grades of neurotoxicity and CRS, detailed neurological symptoms, MRI and FDG-PET data were extracted from our prospective database or patients' charts. EEG findings of 22 patients included in this study have been previously described [9].

EEG

Continuous video-EEG (cEEG), with 21 electrodes arranged after the international 10-20 system, was obtained upon clinician request. As per institutional protocol (**Suppl. Table 1**), cEEGs were requested in patients presenting with neurotoxicity ≥ 2 and in patients with clinical seizures or unexplained focal deficit.

Data entry in the EEG database was prospectively performed by the attending clinical neurophysiologists with training and certification to use the American Clinical Neurophysiology Society Standardized Critical Care EEG Terminology (ACNS) [30]. EEGs of special interest or with missing data were specifically reviewed for purpose of the study.

To account for potential fluctuations during long-term recording, we selected the EEG recording most proximal to the day in which neurotoxicity reached its peak. EEG background activity was assessed for: presence of PDR; predominant EEG frequency; EEG continuity categorized as suppressed (<10μV), burst-suppression (suppression >50%), discontinuous (suppression 10-49%) or nearly-continuous (suppression <10%) [30]. Additionally, EEG background was scored using the Synek scale [31] which has previously been validated in a cohort of pediatric CAR T population [13]:

- Grade 1: PDR with alpha-theta slowing
- Grade 2: PDR with predominant theta
- Grade 3: loss of PDR, predominant delta
- Grade 4: burst suppression (BS), discontinuous
- Grade 5: suppression

The presence of slowing or attenuation and their characteristics (focal vs generalized) were recorded.

The presence of electrographic seizures, epileptiform discharges, and RPPs was assessed as well as their features including; prevalence, duration, typical and maximum frequencies, number of phases, sharpness, amplitude, fluctuation or evolution, and plus modifiers. RPP were further categorized as part of IIC in presence of 1) lateralized period discharges (LPD); 2) lateralized rhythmic delta activity (LRDA) with modifiers or frequency 1.5Hz or higher; 3) generalized periodic discharges (GPD) with modifiers or frequency 1.5Hz or higher. Patients who presented with IIC patterns and seizures were included in the IIC group for statistical analysis.

Focal EEG abnormalities were defined as the presence of at least one of the following: LPD, LRDA, lateralized spike-and-wave (LSW), focal seizures, or focal slowing/attenuation.

We assessed the correlation between neurotoxicity grade and presence of RPP; between focal EEG abnormalities and focal clinical deficit; and between neurotoxicity grade and amount of background disorganization scored as per the Synek scale.

Imaging analysis

18-F-fluorodeoxyglucose (18F-FDG) PET/CT of the brain was performed, upon clinical discretion, to assess for a hypermetabolic epileptic focus. 18F-FDG was injected, after a fasting period of at least 4hours, and, after uptake of 45-60 minutes. Images were acquired and analyzed using Hermes Hybrid Viewer PDR (Version 2.6N). MRI perfusion was performed using dynamic susceptibility contrast echo-planar imaging during intravenous gadolinium contrast infusion.

Statistical Methods

Correlations of categorical variables were evaluated by using Wilcoxon or Kruskal-Wallis tests and the Dunn posthoc test. Analysis of binary variables was performed employing Chi-square or Fisher exact tests; continuous variables were assessed by T-test or ANOVA as appropriate. Correlation between neurotoxicity grades and Synek scale or EEG main background frequency was assessed using Spearman's rank correlation test. A correlation of at least 0.8 was considered as very strong, values between 0.6 and 0.7 as strong, between 0.3 and 0.5 as fair, and values <0.3 as no or negligible correlation. The Benjamini-Hochberg (BH) procedure was applied to control for false discovery rate, using a q value of 0.05. Data analysis was performed using R version 4.0.0 (R Foundation for Statistical Computing, Vienna, Austria).

Data Availability Statement

Anonymized data can be shared upon reasonable request, from qualified investigators, by the corresponding author.

Results

We identified 83 patients who underwent cEEG following CAR T treatment. Two patients did not experience neurotoxicity and were excluded from the analysis, resulting in a total of 81 patients with a mean age of 60.4 ± 11.0 years (**Table 1**). The vast majority of the patients presented with lymphoma (77, 95.1%) including 59 diffuse large B cell lymphoma (DLCBL), 6 follicular lymphomas (FL), 5 primary mediastinal B-cell lymphomas (PMBCL), 2 mantle cell lymphoma (MCL), 2 marginal zone lymphoma (MZL) and 3 other Non-Hodgkin's Lymphoma (NHL). Additional 2 patients (2.5%) were treated for acute lymphoblastic leukemia (ALL) and 2 (2.5%) for multiple myeloma (MM). CD19-targeted CAR T cells were infused in 79 (96.2%) of our patients (76 axicabtagene ciloleucel, 1 tisagenlecleucel, 1 JCAR015, 1 brecucabtagene autoleucel) and the two patients with MM received BCMA-targeted CAR T (idecabtagene vicleucel).

All of the patients experienced CRS. Neurotoxicity occurred at a median of 6 days (range 1-34) after CAR T cell infusion. Median peak neurotoxicity grade was 3 (IQR 2-3) with 11 patients (13.58%) presenting with neurotoxicity grade 1, 25 patients (34.6%) with grade 2, 42 patients (51.85%) with grade 3, and 3 patients (3.70%) with grade 4.

cEEGs were not recorded during neurotoxicity peak in 20 patients. Among them, 15 had improved neurotoxicity grades, and 5 had not yet reached neurotoxicity peaks and clinically worsened during the subsequent days (**Fig 1**). Per hospital protocol, 94.8% of our patients were on levetiracetam prophylaxis during cEEG recording.

Head CT scans were performed in 74 (89.2%) patients, of which 67 showed no abnormalities. MRI scans were performed in 41 (49.4%) patients; MRI abnormalities were described in 15 patients consisting of punctate or multiple diffusion restriction concerning for strokes (n=3), hypoperfusion (n=2), new vascular stenosis (n=2), T2/FLAIR hyperintensities (n=4) with extensive cerebral and medullary involvement in one patient, and lesions compatible with CNS lymphoma (n=4) such as leptomeningeal enhancement, ependymal enhancement, or homogeneously enhancing lesion. In addition, 8 (9.88%) patients obtained a PET-CT demonstrating diffuse hypometabolism in 4 patients, lateralized or hemispheric hypometabolism in 3, and no abnormality in one (**Fig 3**). Lumbar punctures (LP) were performed in 19 patients with median neurotoxicity peak 3 (range 1-4). In most cases CSF was either no inflammatory or minimally inflammatory; median total white blood cells 6/uL (IQR 3-27.3, range 0-242) and median protein counts 87 mg/dl (IQR 54.30-125.95, range 9-234.30). We did not find any correlation between neurotoxicity peak and LP findings (p=0.103 for total white blood cell and p=0.607 for protein counts).

cEEG background was continuous in 73 (90.1%) patients, nearly continuous in 5 (6.2%), discontinuous in 2 (2.5%), and suppressed in 1 (1.2%). The three patients with discontinuous and suppressed cEEGs were intubated and sedated with either midazolam or propofol/midazolam which likely have confounded the EEG background assessment.

cEEG main frequency was in the alpha range in 12 (15.4%), theta in 57 (73.1%), delta in 8 (10.3%), and beta in 1 (1.3%), with 3 patients (3.7 %) presenting with asymmetric background activity. Predominant cEEG frequency was significantly correlated to both neurotoxicity peak grade (p=0.001, significant after correction for multiple comparisons) and neurotoxicity grade the day of cEEG recording (p <0.001, significant after correction for multiple comparisons) (**Fig 2**) but not with neurotoxicity duration. Spearman correlation test demonstrated a fair correlation between main cEEG background frequency and neurotoxicity grades the day of cEEG recording (ρ=0.50, 95% CI 0.3-0.7). The posterior dominant rhythm was lost in 36 (44.4%) patients and significantly correlated with more severe neurotoxicity the day of cEEG recording (p=0.003, significant after correction for multiple comparisons) but, not with neurotoxicity peak (p=0.03, significance lost after correction for multiple

comparisons) or neurotoxicity duration (p=0.2). The Median Synek scale was 2 (IQR 2-3) and significantly correlated with higher neurotoxicity grades the day of cEEG recording (**Table 2**). Spearman correlation test demonstrated a fair correlation between Synek scale and neurotoxicity the day of cEEG recording (ρ=0.42, 95% CI 0.2-0.6).

A total of 42 patients presented with RPP (**Table 1**). On the day of cEEG recording, their median neurotoxicity grade was 2 (IQR 2-3) (**Fig 1**). The most common pattern was generalized rhythmic delta activity (GRDA) in 38 (46.9%) patients, typically at 1.5-2Hz predominant in the anterior region and rarely with "plus" modifiers. Generalized periodic discharges (GPD) were found in 12 (14.8 %) patients, all of them with a triphasic morphology, and 11/12 in the IIC mainly due to a frequency ≥of 1.5 Hz with two patients presenting other modifiers (**Suppl Fig 1**). Neither the presence of periodic or rhythmic patterns as a whole or any specific pattern, significantly correlated with neurotoxicity severity.

Clinical seizures were reported in 6 (7.4%) patients. Three patients had isolated GTCS prior to EEG placement and no further seizures were recorded thereafter. The remaining three patients had clinical episodes suspect of focal seizures; one presented with unambiguous clinical and multiple focal electrographic seizures (**Suppl. Case 4, Fig 3D)** and the other two had cEEG episodes satisfying the modified Young criteria for seizures [30,32], though with uncertain clinical correlation (**Suppl. Cases 1 and 3, Fig 3A&B**). Additionally, 8 (9.9%) patients demonstrated epileptiform discharges and one patient had GSW (**Fig 3).** Among them 4/9 had electro-clinical seizures, 1/9 had clinical only seizures and 4/4 did not have seizures. Five patients presented focal RPP (4 LRDA, 1 LRDA, and LPD), all in the IIC: one had undoubtful electro-clinical seizures (**Suppl. Case 4, Fig 3D),** two had electrographic seizures with uncertain clinical correlation in two (**Suppl. Cases 1 and 3, Fig 3A&B**) and one patient had LRDA associated with delta slowing of shifting lateralization (**Suppl. Case 5, Suppl. Fig.1C**). Surprisingly, these three patients with ictal activity presented with brain FDG-PET hypometabolism (**Fig 3**). All patients with focal RPP presented with focal symptoms with the lateralization of symptoms congruent with the cEEG patterns (**Suppl. Cases 1-4, Table 3**). Besides, 15 patients presented with focal slowing without focal RPP. Of these patients, 6 had focal clinical symptoms co-localizing with EEG slowing. In total, 21 (25.9%) patients had focal cEEG abnormalities, 11 presenting with focal symptoms, and 6 with focal symptoms other than aphasia. Focal RPP were significantly associated with clinical symptoms other than aphasia (p=0.002, significant after correction for multiple comparisons) but not with overall clinical focal symptoms (p=0.03, significance lost after correction for multiple comparisons). Focal slowing/attenuation was not associated with such clinical symptoms (**Table 3, Fig 3**).

After hospital discharge, antiseizure medications (ASMs) were gradually discontinued, no patients continued on ASMs beyond 3 months, and no patient experiencing recurrent seizures. Of note, no patients who presented clinical or electrical seizures had a history of epilepsy.

Patients of special interest are described further in Supplementary Material (**Suppl. cases 1-5**).

Discussion

This study systematically describing cEEGs in a large single-center cohort of patients presenting with neurotoxicity after CAR T treatment confirmed the high prevalence of cEEG abnormalities. Nonspecific, generalized slowing was the most frequently encountered pattern with a good correlation between the amount of cEEG slowing and severity of neurotoxicity. RPPs are also frequently encountered; patients from our cohort demonstrated relatively frequent IIC patterns and focal cEEG abnormalities, sometimes with shifting lateralization. These focal cEEG abnormalities were often associated with congruent focal clinical symptoms, without structural lesion but with unexpected PET hypometabolism or MRI hypoperfusion, raising yet unanswered questions about the mechanisms of neurotoxicity.

In agreement with previous reports, encephalopathy with diffuse cEEG background alterations was the most common findings [9,19,21,22]. cEEG background patterns (both represented by the Synek scale or as cEEG main frequency) significantly correlated with neurotoxicity severity. These results are in line with a pediatric study reporting a strong correlation between the Synek scale, neurotoxicity, and Cornell Assessment of Pediatric delirium[15]. To our knowledge, similar studies have not been performed on adults. These findings suggest that EEG background changes might reflect brain dysfunction during immunotherapy and that EEG background may be a marker for neurotoxicity severity. These findings might however not be specific to CAR T cells neurotoxicity but just represent a non-specific marker of suppressed mental status. Indeed, similar results have been described in patients with delirium [33].

More than half of our population presented with RPPs (56.8 %). Previous studies have reported similar patterns in up to 90% (11/12) of CAR T patients with severe neurotoxicity (grade 3-4) and 50% (3/6) with low-grade neurotoxicity (grade 1-2) mainly consisting of GPD and GRDA [21]. Similarly, a case series of four patients with encephalopathy described clinical worsening occurring in correlation with GPDs peak [20]. In a group of 20 patients with language disturbance, all patients with GRDAs or GPDs had severe neurotoxicity (grade 3-4) [27]. Surprisingly, in our cohort, the presence of RPP did not correlate with the severity of neurotoxicity. This might be explained by the distribution of

neurotoxicity grades among our population with half of our patients presenting with grade 3 neurotoxicity and only 3 with higher grades, or by the retrospective design of our study without simultaneous cEEG and clinical evaluation. However, 22 patients had only low grades neurotoxicity (3 with grade 1, 18 with grade 2) despite the presence of RPP, suggesting that these patterns might not invariably be associated with severe neurotoxicity. Furthermore, at the time of cEEGs recording, 2 patients still exhibited GRDAs despite resolution of neurological symptoms. Among 8 patients with neurotoxicity grade 1, 3 had GPDs and 7 had GRDAs suggesting that cEEGs abnormalities might evolve more slowly than clinical dysfunction.

Even with a restrictive definition of IIC, almost a quarter of our population presented with clear IIC patterns. IIC represents a bridge between ictal and interictal phenomena and has previously been described to be associated with subsequent seizures [34-36]. Although incontrovertible seizures were relatively rarely described in our cohort, patterns within the IIC were common, suggesting a state of atypical cortical irritability. Seizure frequency in this population varies significantly, with most of the existing studies reporting seizure incidence without clinical or EEG description [8,9,13,15,19,21,22,24,26,37,38]. Among the landmark trials, the incidence of seizures varies between 1-4% [8,26,37,39]. Interestingly, in agreement with our experience, some authors report clinical events of involuntary rhythmic movements without EEG correlates [21] suggesting that clinical evaluation might overestimate the incidence of seizures. Little is known regarding the EEG in neurotoxicity after CAR T cells, but previous studies have suggested an association between neurotoxicity and IIC [9,13,20,21,27]. In the previously mentioned case series describing GPDs in four patients with encephalopathy, there was no electro-clinical response after initiation of ASMs; however, the case series did report a sustained electro-clinical improvement in all patients after treatment with dexamethasone [20]. On the other hand, a case series reports improvement of aphasia in 6 patients with GPDs on cEEG after initiation of ASMs, suggesting an ictal component [27]. As a worst outcome has been described in ICU-patients presenting with subclinical seizures [40,41], we would recommend initiating dexamethasone and ASMs in patients presenting with subclinical seizures. In patients showing epileptiform activity or IIC, we would suggest pursuing cEEG monitoring for non-convulsive-seizure assessment and consider initiation of corticosteroids. Importantly, none of our patients developed long-term epilepsy, with ASMs successfully discontinued within 3 months.

FDG-PET has emerged as a method of characterizing the metabolic impact of IIC patterns and serves as a means of evaluating metabolic stress and neuronal injury [42]. In our cohort, among the 8 patients who had FDG-PET, 7 patients presented with RPP, 4 within the IIC. Of these patients, the majority demonstrated diffuse or focal hypometabolism, corresponding to foci of concerning activity seen on EEG. Seizures and RPPs are typically

thought to be associated with PET hypermetabolism/MRI hyperperfusion[42,43]. These patients represent extraordinary challenges to this assumption and may suggest against seizures as a common underlying mechanism of neurotoxicity. However, this is not unique, as chronic periodic lateralized epileptiform discharges have been associated with FDG-PET hypometabolism in patients with anti-NMDAR encephalopathy [44].

A quarter of our cohort presented focal cEEG abnormalities, sometimes with shifting lateralization, without evidence of structural lesions. Interestingly some of these patients demonstrated congruent neurological symptoms with co-localizing FDG-PET hypometabolism or MRI hypoperfusion. Similar focal cEEG abnormalities, without MRI lesions, have been reported in CAR T cell patients who develop aphasia [27]. In a pediatric cohort, focal cEEG abnormalities consisting of LPD, focal spikes, multi-focal seizures, and focal slowing were reported. In contrast to our observations, MRI was frequently described as abnormal, mainly with diffuse T2 hyperintensity and diffusion restriction [13].

The mechanisms underlying CAR T cell neurotoxicity are still poorly understood. One of the potential explanations is that neurotoxicity is the result of cytokine-mediated endothelial dysfunction which, in turn, leads to changes in blood-brain barrier (BBB) permeability [19,45]. Theoretically, regional cerebral endothelial dysfunction could account for periods of both focal and generalized symptoms and in severe cases, this disruption could lead to the diffuse and often fatal cerebral edema that has been reported [19,22,46]. As BBB dysfunction leads to astrocyte dysfunction and neuronal hypersynchrony and may contribute to epileptogenesis, this may explain the RPP and IIC patterns found in our patients [47]. Furthermore, as BBB increased permeability would disrupt the homeostasis of extra-cellular contents leading to potential cortical spreading depression which could account for the clinical reversible neurological symptoms, the cortical PET-hypometabolism, and some of the EEG abnormalities.

This study has several limitations. Due to the retrospective design of the study, cEEGs and images were obtained upon clinical discretion, without a control group of asymptomatic patients. Strong correlations are therefore difficult to establish. Functional images (FDG-PET, perfusion-MRI) were obtained mainly in patients presenting with focal neurological symptoms or focal cEEG abnormalities. Due to this selection bias, it is difficult to conclude whether the reported hypoperfusion/hypometabolism is directly related to the focal clinical findings or occur more widely in neurotoxicity, or even in patients who received CAR T cells treatment without resultant neurotoxicity. As cEEGs were recorded only during neurotoxicity with no prior or subsequent EEG recording, it is impossible to exclude that the patients had baseline EEG alterations not related to neurotoxicity. This is especially true in our 5 patients who had MRI lesions highly suggestive of CNS involvement of their lymphoma, 2 of them with diagnosis confirmed after lumbar puncture. However, the strong

correlations found between cEEGs background alterations and neurotoxicity grade, as well as cEEGs improvement after steroids treatment described in some of our patients, mitigate this possibility. Because cEEGs were performed upon clinical indication, cEEGs were not obtained in the pre-symptomatic stage necessary for neurotoxicity occurrence or severity prediction. Of note, five patients had cEEG recordings before neurotoxicity reached its peak. Among them one with neurotoxicity grade 1 presented with GPDs within the IIC (Suppl. Figure 1A) and two with neurotoxicity grade 1 hade Synek scale grade 3. These data may suggest that EEG could help to predict neurotoxicity worsening. Further prospective studies investigating EEG prediction performance are required. Nevertheless, we consider still important to characterize the range of abnormalities seen on EEG in this population and their correlation to neurological status.

Our population is not homogeneous and includes patients with various types of cancer and treated with different CAR T constructs. Reported clinical symptoms of neurotoxicity slightly differ between the different CAR T products and we cannot exclude that cEEG might as well. As the vast majority of our population was treated with axicabtagene ciloleucel (Yescarta) and presented with DLCBL, our sample size was unfortunately too small to allow comparison between tumor type or CAR T products. We decide to include all patients and not restrict to one specific CAR T product or one oncological diagnosis, to provide the best representation of what neurological consultants might face in a real-life situation. We did not always have a close temporal relationship between cEEGs recording and clinical evaluation and therefore were not able to assess the evolution of clinical symptoms in comparison with EEG. The Synek scale was originally designed for prognosis assessment in traumatic or anoxic encephalopathies [31] but has later been used in more similar clinical situations such as septic encephalopathy [48] and pediatric neurotoxicity after CAR T cells [13]. As this scale was previously used in a pediatric CAR T population, we decided to use it to facilitate standardized comparisons. As a large part of our population was treated before the introduction of the ICANS neurotoxicity criteria [7], neurotoxicity was graded according to an adapted version of the NCI CTCAE v4.03 which may limit the generalization of our results for further studies. This problem is unfortunately recurrent in CAR T studies and led to the development of the ICANS scale. However, as our main aim was to systematically describe EEGs and study their correlation with clinical and radiological findings, we studied the largest population available to us. The CTCAE scale deviated from the ICANS mainly because it integrates headaches, and isolated seizures are scored grade 2. However, every patient experiencing seizures was retrospectively scored as neurotoxicity grade ≥ 2 and in our adapted version, isolated headaches were not considered neurotoxicity. This should improve the generalizability of our results and mitigate the possibility that patients experiencing neurological symptoms (headaches) not related to neurotoxicity were included.

In conclusion, this study demonstrates that cEEG background alterations are correlated with neurotoxicity grade, offering the possibility to use EEG, a non-invasive and widely available tool, to monitor neurotoxicity severity. Further prospective studies are required to investigate the possibility to use EEG to monitor neurotoxicity severity and to determine the timing of EEG changes in relation to clinical symptoms to facilitate the potential use of EEG to monitor neurotoxicity occurrence, duration, and response to treatment. Furthermore, our data highlight the relatively frequent occurrence of IIC and focal EEG abnormalities, with congruent focal neurological symptoms, with co-localizing PET hypometabolism or MRI hypoperfusion. These data raised significant questions regarding neurotoxicity pathophysiology; the utility of escalating ASM these patients remains unclear.

Bibliography

1. Brudno JN, Kochenderfer JN. Chimeric antigen receptor T-cell therapies for lymphoma. *Nat Rev Clin Oncol.* 2018; 15(1):31-46.
2. Rosenberg SA, Restifo NP. Adoptive cell transfer as personalized immunotherapy for human cancer. *Science.* 2015; 348(6230):62-68.
3. Jackson HJ, Rafiq S, Brentjens RJ. Driving CAR T-cells forward. *Nat Rev Clin Oncol.* 2016; 13(6):370-383.
4. Hinrichs CS, Rosenberg SA. Exploiting the curative potential of adoptive T-cell therapy for cancer. *Immunol Rev.* 2014; 257(1):56-71.
5. Maude SL, Frey N, Shaw PA, et al. Chimeric antigen receptor T cells for sustained remissions in leukemia. *N Engl J Med.* 2014; 371(16):1507-1517.
6. Gutierrez C, McEvoy C, Mead E, et al. Management of the Critically Ill Adult Chimeric Antigen Receptor-T Cell Therapy Patient: A Critical Care Perspective. *Crit Care Med.* 2018; 46(9):1402-1410.
7. Lee DW, Santomasso BD, Locke FL, et al. ASTCT Consensus Grading for Cytokine Release Syndrome and Neurologic Toxicity Associated with Immune Effector Cells. *Biol Blood Marrow Transplant.* 2019; 25(4):625-638.
8. Neelapu SS, Locke FL, Bartlett NL, et al. Axicabtagene Ciloleucel CAR T-Cell Therapy in Refractory Large B-Cell Lymphoma. *N Engl J Med.* 2017; 377(26):2531-2544.
9. Rubin DB, Danish HH, Ali AB, et al. Neurological toxicities associated with chimeric antigen receptor T-cell therapy. *Brain.* 2019; 142(5):1334-1348.
10. Brudno JN, Kochenderfer JN. Toxicities of chimeric antigen receptor T cells: recognition and management. *Blood.* 2016; 127(26):3321-3330.
11. Teachey DT, Lacey SF, Shaw PA, et al. Identification of Predictive Biomarkers for Cytokine Release Syndrome after Chimeric Antigen Receptor T-cell Therapy for Acute Lymphoblastic Leukemia. *Cancer Discov.* 2016; 6(6):664-679.
12. Davila ML, Riviere I, Wang X, et al. Efficacy and toxicity management of 19-28z CAR T cell therapy in B cell acute lymphoblastic leukemia. *Sci Transl Med.* 2014; 6(224):224ra225.
13. Gust J, Annesley CE, Gardner RA, Bozarth X. EEG Correlates of Delirium in Children and Young Adults With CD19-Directed CAR T Cell Treatment-Related Neurotoxicity. *J Clin Neurophysiol.* 2019.
14. Park JH, Riviere I, Gonen M, et al. Long-Term Follow-up of CD19 CAR Therapy in Acute Lymphoblastic Leukemia. *N Engl J Med.* 2018; 378(5):449-459.
15. Gust J, Taraseviciute A, Turtle CJ. Neurotoxicity Associated with CD19-Targeted CAR-T Cell Therapies. *CNS Drugs.* 2018.
16. Neelapu SS, Tummala S, Kebriaei P, et al. Chimeric antigen receptor T-cell therapy - assessment and management of toxicities. *Nat Rev Clin Oncol.* 2018; 15(1):47-62.
17. Rice J, Nagle S, Randall J, Hinson HE. Chimeric Antigen Receptor T Cell-Related Neurotoxicity: Mechanisms, Clinical Presentation, and Approach to Treatment. *Curr Treat Options Neurol.* 2019; 21(8):40.
18. Rubin DB, Al Jarrah A, Li K, et al. Clinical Predictors of Neurotoxicity After Chimeric Antigen Receptor T-Cell Therapy. *JAMA Neurol.* 2020.
19. Gust J, Hay KA, Hanafi LA, et al. Endothelial Activation and Blood-Brain Barrier Disruption in Neurotoxicity after Adoptive Immunotherapy with CD19 CAR-T Cells. *Cancer Discov.* 2017; 7(12):1404-1419.
20. Herlopian A, Dietrich J, Abramson JS, Cole AJ, Westover MB. EEG findings in CAR T-cell therapy-related encephalopathy. *Neurology.* 2018; 91(5):227-229.
21. Karschnia P, Jordan JT, Forst DA, et al. Clinical presentation, management, and biomarkers of neurotoxicity after adoptive immunotherapy with CAR T cells. *Blood.* 2019; 133(20):2212-2221.

22. Santomasso BD, Park JH, Salloum D, et al. Clinical and Biological Correlates of Neurotoxicity Associated with CAR T-cell Therapy in Patients with B-cell Acute Lymphoblastic Leukemia. *Cancer Discov.* 2018; 8(8):958-971.

23. Belin C, Devic P, Ayrignac X, et al. Description of neurotoxicity in a series of patients treated with CAR T-cell therapy. *Sci Rep.* 2020; 10(1):18997.

24. Gofshteyn JS, Shaw PA, Teachey DT, et al. Neurotoxicity after CTL019 in a pediatric and young adult cohort. *Ann Neurol.* 2018; 84(4):537-546.

25. Maude SL, Laetsch TW, Buechner J, et al. Tisagenlecleucel in Children and Young Adults with B-Cell Lymphoblastic Leukemia. *N Engl J Med.* 2018; 378(5):439-448.

26. Schuster SJ, Investigators J. Tisagenlecleucel in Diffuse Large B-Cell Lymphoma. Reply. *N Engl J Med.* 2019; 380(16):1586.

27. Sokolov E, Karschnia P, Benjamin R, et al. Language dysfunction-associated EEG findings in patients with CAR-T related neurotoxicity. *BMJ Neurology Open.* 2020; 2(1).

28. Lee DW, Gardner R, Porter DL, et al. Current concepts in the diagnosis and management of cytokine release syndrome. *Blood.* 2014; 124(2):188-195.

29. Services. USDoHH. Common Terminology Criteria for Adverse Events (CTCAE) Version 4.0. 2010.

30. Hirsch LJ, LaRoche SM, Gaspard N, et al. American Clinical Neurophysiology Society's Standardized Critical Care EEG Terminology: 2012 version. *J Clin Neurophysiol.* 2013; 30(1):1-27.

31. Synek VM. Prognostically important EEG coma patterns in diffuse anoxic and traumatic encephalopathies in adults. *J Clin Neurophysiol.* 1988; 5(2):161-174.

32. Young GB, Jordan KG, Doig GS. An assessment of nonconvulsive seizures in the intensive care unit using continuous EEG monitoring: an investigation of variables associated with mortality. *Neurology.* 1996; 47(1):83-89.

33. Kimchi EY, Neelagiri A, Whitt W, et al. Clinical EEG slowing correlates with delirium severity and predicts poor clinical outcomes. *Neurology.* 2019; 93(13):e1260-e1271.

34. Chong DJ, Hirsch LJ. Which EEG patterns warrant treatment in the critically ill? Reviewing the evidence for treatment of periodic epileptiform discharges and related patterns. *J Clin Neurophysiol.* 2005; 22(2):79-91.

35. Osman GM, Araujo DF, Maciel CB. Ictal Interictal Continuum Patterns. *Curr Treat Options Neurol.* 2018; 20(5):15.

36. Rodriguez Ruiz A, Vlachy J, Lee JW, et al. Association of Periodic and Rhythmic Electroencephalographic Patterns With Seizures in Critically Ill Patients. *JAMA Neurol.* 2017; 74(2):181-188.

37. Maude SL. Tisagenlecleucel in pediatric patients with acute lymphoblastic leukemia. *Clin Adv Hematol Oncol.* 2018; 16(10):664-666.

38. Turtle CJ, Hanafi LA, Berger C, et al. CD19 CAR-T cells of defined CD4+:CD8+ composition in adult B cell ALL patients. *J Clin Invest.* 2016; 126(6):2123-2138.

39. Locke FL, Ghobadi A, Jacobson CA, et al. Long-term safety and activity of axicabtagene ciloleucel in refractory large B-cell lymphoma (ZUMA-1): a single-arm, multicentre, phase 1-2 trial. *Lancet Oncol.* 2019; 20(1):31-42.

40. De Marchis GM, Pugin D, Meyers E, et al. Seizure burden in subarachnoid hemorrhage associated with functional and cognitive outcome. *Neurology.* 2016; 86(3):253-260.

41. Payne ET, Zhao XY, Frndova H, et al. Seizure burden is independently associated with short term outcome in critically ill children. *Brain.* 2014; 137(Pt 5):1429-1438.

42. Struck AF, Westover MB, Hall LT, Deck GM, Cole AJ, Rosenthal ES. Metabolic Correlates of the Ictal-Interictal Continuum: FDG-PET During Continuous EEG. *Neurocrit Care.* 2016; 24(3):324-331.

43. Vespa PM, McArthur DL, Xu Y, et al. Nonconvulsive seizures after traumatic brain injury are associated with hippocampal atrophy. *Neurology.* 2010; 75(9):792-798.

44. Sakakibara E, Takahashi Y, Murata Y, Taniguchi G, Sone D, Watanabe M. Chronic periodic lateralised epileptic discharges and anti-N-methyl-D-aspartate receptor antibodies. *Epileptic Disord.* 2014; 16(2):218-222.

45. Norelli M, Camisa B, Barbiera G, et al. Monocyte-derived IL-1 and IL-6 are differentially required for cytokine-release syndrome and neurotoxicity due to CAR T cells. *Nat Med.* 2018; 24(6):739-748.

46. Schuster SJ, Svoboda J, Chong EA, et al. Chimeric Antigen Receptor T Cells in Refractory B-Cell Lymphomas. *N Engl J Med.* 2017; 377(26):2545-2554.

47. Friedman A, Heinemann U. Role of Blood-Brain Barrier Dysfunction in Epileptogenesis. In: th, Noebels JL, Avoli M, Rogawski MA, Olsen RW, Delgado-Escueta AV, eds. *Jasper's Basic Mechanisms of the Epilepsies*. Bethesda (MD)2012.

48. Azabou E, Magalhaes E, Braconnier A, et al. Early Standard Electroencephalogram Abnormalities Predict Mortality in Septic Intensive Care Unit Patients. *PLoS One.* 2015; 10(10):e0139969.

Table

Table 1: Comparison of clinical characteristics between the whole population and patients presenting with rhythmic/periodic patterns or patterns within the ictal-interictal continuum.

Table 2: Distribution of EEG scored according to the Synek scale

Table 3: Characteristics of patients with focal EEG who had cerebral images

Figure's legend:

Figure 1: Distribution of neurotoxicity grades in patients with EEGs demonstrating rhythmic or periodic pattern (RPP), in patients with EEGs showing patterns within the ictal-interictal continuum (IIC), and in patients without IIC or RPP. The X-axis shows peak neurotoxicity grade (**A**) or neurotoxicity grade on the day of EEG recording (**B**). Y-axis shows patient's percentage. Neither presence of RPPs as a whole nor IIC significantly correlated with neurotoxicity severity (for all p>0.005).

Figure 2: EEG background correlates with clinical neurotoxicity severity. The X-axis shows the EEG background main frequency (**A**) or Synek scale grade (**B)**, and the y-axis shows the neurotoxicity grade on the day of the EEG recording. Each data point represents an individual. Post-hoc analyses with Wilcoxon test were performed and adjusted p-value are represented. EEG background main frequency was not available (NA) in three patients with suppressed or discontinuous EEG.

Figure 3: MRI perfusion and FDG-PET in patients with focal EEG abnormalities/focal clinical symptoms.

EEGs are presented in a longitudinal bipolar montage (left-left-midline-right-right-ECG), sensitivity 7μV/mm (besides figures C where sensitivity is 30μV/mm), time base 30 mm/s, low-frequency filter 1Hz, high-frequency filter 70 Hz, notch 60Hz. The scale is provided with an x-axis showing time (s) and a y-axis showing voltage amplitude (μV)

A (Patient previously described [9]**):** The patient presented with aphasia and agitated delirium followed 5 days later by brief episodes of marching arm and face numbness associated with scotoma, that switch laterality. His history is described in **suppl. case 1**. **A1**: Brain FDG-PET, demonstrates focal right parieto-temporal hypometabolism. **A2-3**: EEG shows abnormalities of shifting lateralization with right evolving 2.5 Hz LRDA (**A2**) followed the next day by left delta slowing (**A3**).

B (Patient previously described [9]**):** The patients presented with aphasia. **B:** The patients presented with aphasia. **B1-2:** Axial MRI perfusion sequences (**B1** Maximum of Slope

Decrease, **B2** Mean Time to Enhance) demonstrate left parieto-occipital hypoperfusion. **B3**: EEG shows theta-delta slowing over the left hemisphere, predominant over the left temporal region.

C: The patient presented with aphasia, flexor posturing, myoclonus, and decreased level of consciousness. No correlation between abnormal movements and EEG was found. The patient's history is described **in suppl. case 3**. **C1:** Brain FDG-PET, recorded the same day as EEG in **C4-5**, reveals global hypometabolism. **C2**: Coronal-FLAIR cerebral-MRI shows hyperintensity over the medial aspect of both temporal lobes extending anteriorly along the temporal horn. **C3**: T2 sagittal MRI over the upper medullar cord shows extensive cerebral and thoracic hyperintensity **C4-5**: EEG shows continuous, high-voltage, frontal generalized spike and waves (GSW) at 1.5-2.5Hz with bifrontal runs that evolve in morphology and transition to a rhythmic delta, then to 1Hz generalized periodic discharges (episodes satisfies the modified Young criteria for nonconvulsive seizures and last up to 1 min).

D: The patient presented with sequential occurrences of headache, attention deficit, confusion extreme olfactory sensation, visual distortion, and generalized tonic-clonic seizures. Subsequently, despite loading with lorazepam and levetiracetam, he presented with multiple focal seizures (starting with left boding shaking, then generalizing the right-side). The patient's history is described in **suppl. case 4**.**D1:** Brain FDG-PET, recorded the same day as EEG in **D3**, shows mild diffuse hypometabolism. **D2-3**: Initial EEG (**D2**) showed multiple (up to 30 daily) right temporal seizures. After 13 days (patient asymptomatic for 3 days with ongoing down titration of anti-seizure medications), EEG shows persistent right temporal LRDA and LPD (**D3**).

E (Patient previously described [9]**):** The patient presented neurotoxicity grade 3 with right hemiparesis, with complete recovery after 9 days. **E1:** Brain FDG-PET shows left frontal and caudate decreased FDG uptake. **E2**: Axial MRI perfusion sequences (Negative Enhancement Integral) show global decreased perfusion over the left hemisphere. **E3**: EEG shows delta slowing after the left hemisphere with preserve PDR in the alpha range over the right hemisphere.

Table 1: Comparison of clinical characteristics between the whole population and patients presenting with rhythmic/periodic patterns or patterns within the ictal-interictal continuum.

	Whole population	Rhythmic/Periodic patterns		IIC		test
	N= 81	N = 42 (51.9%)	p, OR 95%CI	N = 16 (19.8 %)	p, OR 95%CI	
Female (n, %)	29 (35.8)	15 (35.7)	1 OR 1.0 (0.4-	7 (43.8)	0.56 OR 0.7 (0.2-	Fisher
Age, years (mean, SD)	60.40 ±10.99	60.1 ±11.0	0.79	59.9 ±11.3	0.86	T Test
CRS peak grade (med, IQR)	2 (1-2)	2 (1-2)	0.46	2 (1-2)	0.78	U test
Neurotoxicity delay after infusion, day	6 (5-8)	6 (5-7)	0.82	7 (5-8.25)	0.31	U test
Neurotoxicity peak grade (med, IQR)	3 (2-3)	3 (2-3)	0.58	3 (2-3)	0.13	U test
Neurotoxicity grade day EEG (med, IQR)	2 (1-3) *	2 (2-3)	0.38	2.5 (2-3)	0.06	U test
Neurotoxicity duration, days (med,	9 (6.5-15-0) ***	9 (7-17.5) **	0.21	8.5 (7-12.5) *	0.9	U test
MRI abnormalities (n, %)	15/41 (36.6)	12/27 (44.4)	0.18 OR 0.3 (0.05-	5/12 (41.7)	0.73 OR 0.7 (0.1-	Fisher
Acute CT abnormalities (n, %)	7/74 (9.5)	4/38 (10.5)	1 OR 0.8 (0.1-	2/16 (12.5)	0.64 OR 0.7 (0.09-	Fisher
PET-CT abnormalities (n, %)	7/8 (87)	5/6 (83.3)		4/5 (80)		
Focal clinical symptoms (n, %)	42 (51.85)	29 (69.1)	0.002[b] OR 4.4 (1.6-	13 (81.3)	0.01 OR 5.3 (1.3-	Fisher
Clinical seizures (n, %)	5 (6.2)	4 (9.5)	0.23 OR 5.0 (0.5-	3 (18.8)	0.01 OR 10 (1.3-	Fisher
Received steroids (n, %)	65 (80.3) °	31 (73.8)	0.17 OR 0.4 (0.1-	12 (75)	0.73 OR 0.7 (0.2-	Fisher
Received tocilizumab (n, %)	70 (86.4)	36 (85.7)	1 OR 0.9 (0.2-	13 (81.3)	0.45 OR 0.6 (1.2-	Fisher
Received siltuximab (n, %)	4 (4.9)	3 (7.1)	0.62 OR 2.9 (0.2-	3 (18.8)	0.03 OR 14.1 (1.0-	Fisher
Received Anakinra (n, %)	2 (2.3)	2 (4.8)		2 (12.5)		

*1missing data ** 4 missing data*** 5 missing data IIC: Ictal Interictal Continuum
[b]Significant after Benjamini-Hochberg's correction.

Table 2: Distribution of EEG scored according to the Synek scale

	Synek scale 1 N = 17 (21%)	Synek scale 2 N = 29 (35.8%)	Synek scale 3 N = 32 (39.5%)	Synek scale 4 N = 2 (2.5%)	Synek scale 5 N =1 (1.2%)	P	Test
Female, n (%)	6 (35.3%)	11 (37.9%)	11 (34.4%)	1 (50%)	0 (0%)	0.99	Fisher
Age, years (mean ± SD)	60.5 ± 9.4	62.8 ± 9.8	58.4 ± 12.6	60 ±17.0	55 ± 0	0.33	ANOVA
CRS peak grade (med, IQR)	2 (1-2)	2 (1-2)	2 (1-2)	3 (2.5-3.5)	5	0.20	Kruskal
Neurotoxicity delay after infusion, day (med, IQR)	6 (5.9)	6 (5-7)	6 (5-8)	9 (8-10)	4	0.36	Kruskal
Neurotoxicity peak grade (med, IQR)	2 (1-3)	3 (2-3)	3 (2-3)	4 (4-4)	3	0.01[b]	Kruskal
Neurotoxicity grade the day of EEG (med, IQR)	1 (1-2)	1 (1-2)	3 (2-3)	4 (4-4)	3	0.001[b]	Kruskal
Neurotoxicity duration, day (med, IQR)	8.5 (2.8-13.3) *	9 (5-15) **	9 (7-14) ***	37.5 (28.8-46.3)	8	0.35	Kruskal

*1 missing data ** 4 missing data*** 5 missing data
[b]Significant after Benjamini-Hochberg's correction.

Table 3: Characteristics of patients with focal EEGs who had cerebral images

Patients	EEG	Structural MRI/CT	Perfusion MRI / PET	Clinic
Ictal EEG				
1 (Fig 3A, Suppl. case 1)	Right frontal evolving 3Hz LRDA spreading to the posterior and contralateral lead, followed by LRDA and hemispheric slowing with shifting	CT: Normal	PET: hypometabolism in the right posterior temporal and parietal lobes	Left visual field deficit, sensory disturbance over left arm
2 (Fig 3D, Suppl. case 4)	Multiple right temporal seizures with right temporal LPDs at 2.5-3Hz occurring in cluster and right LRDA and right temporal slowing	MRI: Normal	PET: bilateral hemispheric hypometabolism	Right focal seizure with secondary GTC
3 (Fig 3C, Suppl. case 3)	Continuous 1.5-2.5 Hz GSW with bifrontal runs that evolved in morphology and transition to rhythmic delta, then to 1Hz GPD	MRI: T2-FLAIR hyperintensity over both temporal lobes and the medullar cord	PET: global hypometabolism	Aphasia, flexor posturing, myoclonus, decreased level of consciousness. No correlation between
Focal slowing				
4	Left temporal slowing	MRI: Normal		Aphasia
5 (Fig 3B)	Left hemispheric slowing.	MRI: Normal	MRI: Left parieto-occipital hypoperfusion	Aphasia
6	Right central and frontal slowing.	MRI: Normal		No focal symptom
7	Left temporal slowing.	CT: Normal		No focal symptom
8	Right temporal slowing, multifocal sporadic epileptiform discharges over	CT: Normal		No focal symptom
9	Left temporal slowing.	MRI: non-evolving parafalcine T2 signal		No focal symptom
10	Slowing shifting between the right and left hemispheres.	MRI: Normal		No focal symptom
11	Shifting slowing over left temporal, left occipital, and right parietal, right	CT: Normal		No focal symptom
12	Right hemispheric slowing.	CT: Normal		Left neglect
13 (Fig 3E)	Left hemispheric slowing	MRI: Normal	MRI: Diffuse left-hemispheric hypoperfusion PET: Asymmetric decreased FDG uptake in	Right hemiparesis involving the face
Focal RPP				
14	Very brief 2Hz, left frontal LDRA	MRI: Punctiform stroke in the left MCA territory		Transient language disturbance
15 (Suppl Fig 1C, Suppl. case	Hemispheric delta slowing and LRDA with shifting laterality	MRI: Subtle T2/FLAIR prolongation within the periventricular white matter and the bilateral		Aphasia, Left neglect.
Focal slowing/RPP and GPDs				
16 (Fig 4C, Suppl. Case 2)	GPDs with triphasic morphology, sharp components at times reaching a frequency of 2-3Hz and becoming rhythmic. Brief left temporal LRDA up	CT: Known leptomeningeal enhancement (MRI not repeated), multiple osteolytic metastases.		Agitated delirium, speech difficulty
17	Left temporal slowing, brief evolving 1-2Hz GPD	MRI: leptomeningeal enhancement		Aphasia
18	Frequent GPD, 1.5Hz with a triphasic and sometimes sharply morphology.Abundant 1.5-2.5Hz GRDA.	CT: Non-evolving left frontal oligodendroglioma.		Aphasia
19	Evolving, stimulus-responsive, 1-2Hz GPD. Left temporal delta slowing	MRI: Non-evolving left ethmoidal mass involving the frontal lobe of		Aphasia

RPP: Rhythmic and Periodic Pattern. LRDA: lateralized rhythmic delta activity. GPD: Generalized Periodic discharge. GRDA: Generalized rhythmic delta activity. MCA: Middle Cerebral Artery. GTC: Generalized Tonic-Clonic Seizures. GSW: Generalized Spikes and Waves. Patients 1, 5, 7, and 13 have been previously described [9]

Figure 1

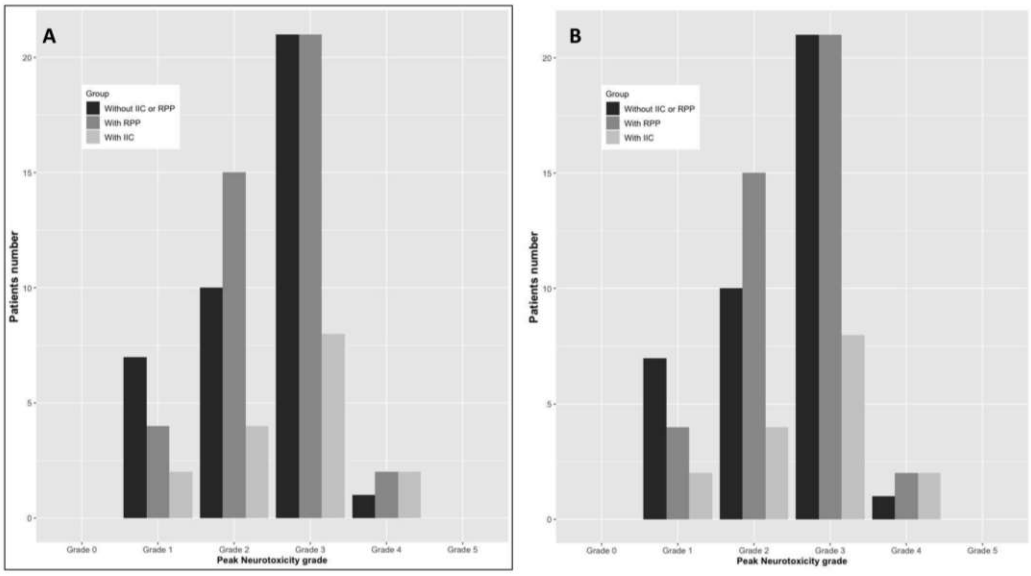

Figure 2

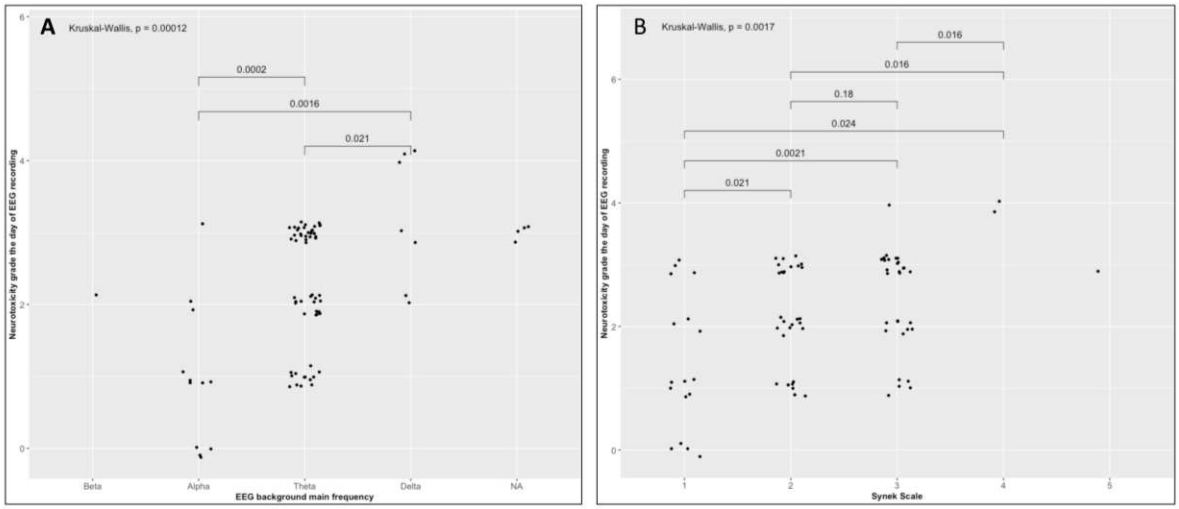

Figure 3